

Polymerizable Vancomycin Derivatives for Bactericidal Biomaterial Surface Modification: Structure–Function Evaluation

McKinley C. Lawson,^{†,‡} Richard Shoemaker,[§] Kevin B. Hoth,[†] Christopher N. Bowman,[†] and Kristi S. Anseth^{*,†,||}

Department of Chemical and Biological Engineering, University of Colorado, Boulder, CO 80309, Medical Scientist Training Program (M.D./Ph.D. Program), University of Colorado School of Medicine, Denver, CO 80220, Department of Chemistry and Biochemistry, University of Colorado, Boulder, CO 80309, Howard Hughes Medical Institute, University of Colorado, Boulder, CO 80309

Received April 11, 2009; Revised Manuscript Received June 6, 2009

Surface modification of implantable biomaterials with biologically active functionalities, including antimicrobials, has wide potential for addressing implant-related design problems. Here, four polymerizable vancomycin derivatives bearing either acrylamide or poly(ethylene glycol) (PEG)-acrylate were synthesized and then polymerized through a surface-mediated reaction. Functionalization of vancomycin at either the V₃ or the X₁ position decreased monomeric activity by 6–75-fold depending on the modification site and the nature of the adduct ($P < 0.08$ for all comparisons). A 5000 Da PEG chain showed an order of magnitude decrease in activity relative to a 3400 Da counterpart. Molecular dynamics computational simulations were used to explore the mechanisms of this decreased activity. Assays were also conducted to demonstrate the utility of a living radical photopolymerization to create functional, polymeric surfaces with these monomers and to demonstrate surface-based activity against *Staphylococcus epidermidis*. In particular, the vancomycin–PEG-acrylate derivatives demonstrated a 7–8 log reduction in bacterial colony forming units (CFU) with respect to nonfunctionalized control surfaces.

Introduction

The function of implantable biomaterials is in large part governed by material surface characteristics, and chemical modification with pharmaceutically inspired polymers at the implant–tissue interface is an attractive option for addressing various biological problems such as postsurgical infection. As newly engineered biomaterials find their way into clinical usage, issues related to the treatment and prevention of foreign-body-related bacterial and fungal infections will continue, and new challenges may be encountered as novel biomaterial–tissue interfaces are designed and characterized.¹ Polymerizable derivatives of traditional antibiotics offer the potential for functionalizing various biomedical materials with the intent of killing local pathogenic organisms. These chemical species, as a class, potentially provide great flexibility for engineering surface architecture, which is thought to strongly influence properties such as protein adsorption, cell adhesion (native and pathogenic), and osteointegration.^{2–4} However, to immobilize these species onto surfaces, one must consider conjugation methods in addition to monomeric structural characteristics.

A wide assortment of antibacterial polymers exists, but the majority are based on various inorganic functionalities rather than on classical, internally administered therapeutics. Most rely on cationic functionalities that interfere with microbial cell membranes and ultimately cause release of cellular constituents (ion leakage) and cell death; phosphonium (P⁺HR₃),^{5–7} and

quaternary amine (N⁺HR₃)^{7–11} functionalities are common. Polymers presenting phenol derivatives^{12–14} and polycationic chitosan polymers^{15,16} have also been synthesized. N-halamine-containing polymers that transfer oxidative halogens (Cl⁺ or Br⁺) directly to cell membranes and cause rapid cell death also exist.^{17–20} While these materials ultimately may be useful for functionalizing implantable biomaterials, it is likely that safety issues related to host cellular toxicity will continue to be of concern.

Examples of synthetic polymers based on traditional antimicrobials include fluoroquinolones,^{21–24} various antifungals,^{25–27} ampicillin,²⁸ and vancomycin.^{29–31} However, with the exception of the vancomycin-based platforms, these approaches presumably rely on the release of active species (i.e., parent drug or polymer degradation products). Thus, there has been little need to define monomer and polymer architectures important for presenting polymerized antibiotic species to microbial cells. Such features are particularly important when the antibacterial system is designed to act through a contact-mediated mechanism independent of chemical elution, such as in the vancomycin-based platform described here.

Vancomycin is the prototypical glycopeptide antibiotic, and it remains potent against gram-positive organisms commonly encountered in association with indwelling medical devices (*Staphylococcus spp.*) such as orthopedic hardware, although resistance can occur.³² It derives its activity from binding D-Ala-D-Ala repeats found at the terminal end of peptidoglycan precursors. Vancomycin blocks the action of both transglycosylases and transpeptidases by complexing with their substrates and preventing proper cross-linking of peptidoglycan structures in the bacterial cell wall.³³ Vancomycin forms several hydrogen bonds with D-Ala-D-Ala peptidoglycan precursors (Figure 1A), and internalization is not required for activity. Many glycopep-

* Author to whom correspondence should be addressed. Tel.: (303) 492-7471. Fax: (303) 735-0095.

[†] Department of Chemical and Biological Engineering, University of Colorado.

[‡] University of Colorado School of Medicine.

[§] Department of Chemistry and Biochemistry, University of Colorado.

^{||} Howard Hughes Medical Institute, University of Colorado.

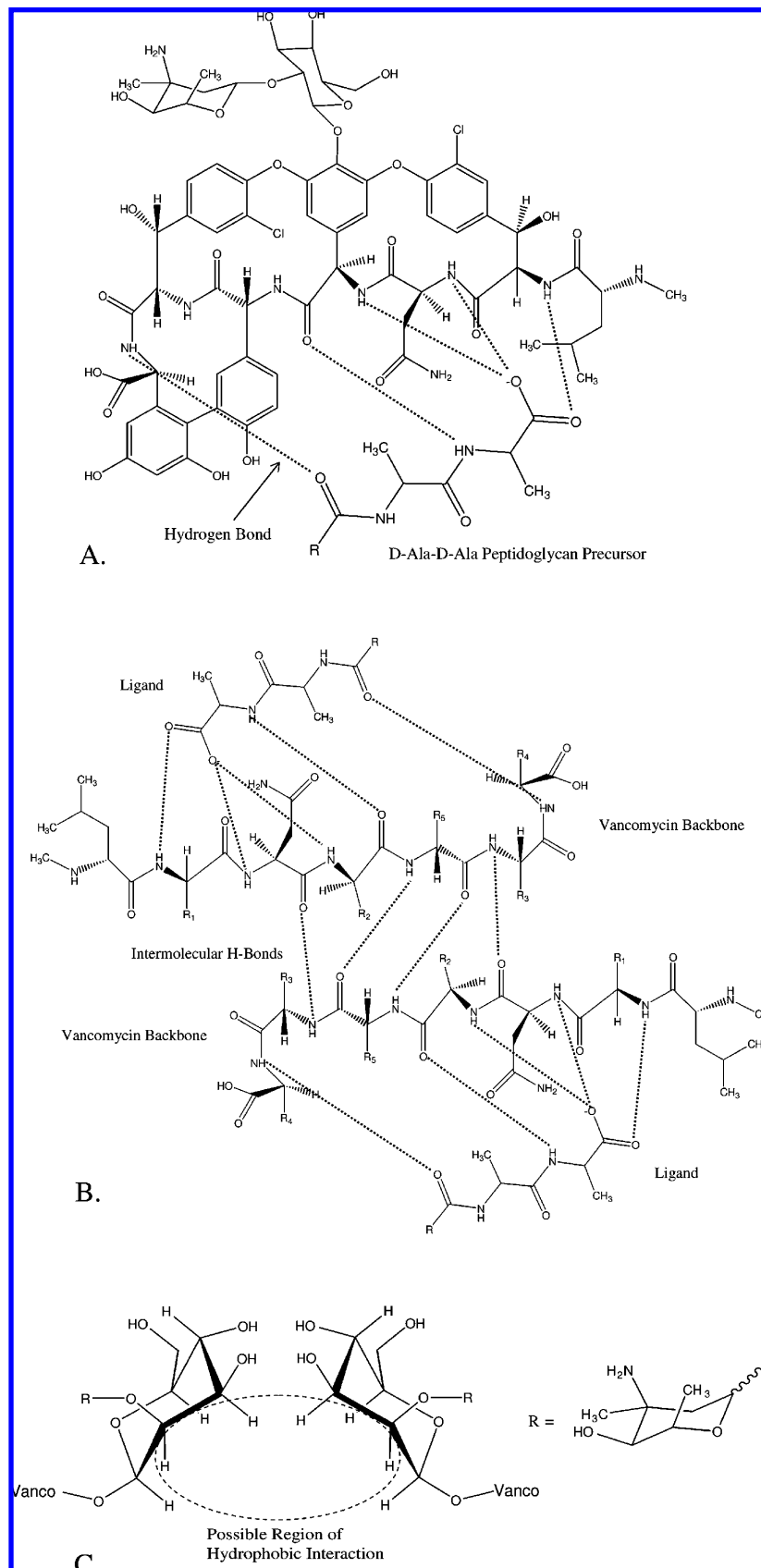


Figure 1. (A) Vancomycin forms multiple hydrogen bonds (dashed lines) with bacterial peptidoglycan precursors and blocks the action of transpeptidases and transglycosylases. (B) Higher-order interactions also play a role in the mechanism of action. Dimers formed through hydrogen bonds along the peptide backbone allow for cooperative substrate binding effects. (C) It has been suggested that hydrophobic interactions between glucose unit C-H groups also play a role in dimer stabilization.

tides form dimers that increase antibiotic potency.^{33–37} These dimers involve intermolecular hydrogen-bonds between adjacent

peptide backbones (Figure 1B) as well as interactions between sugar residues (Figure 1C).^{33–35,37} It has been suggested that

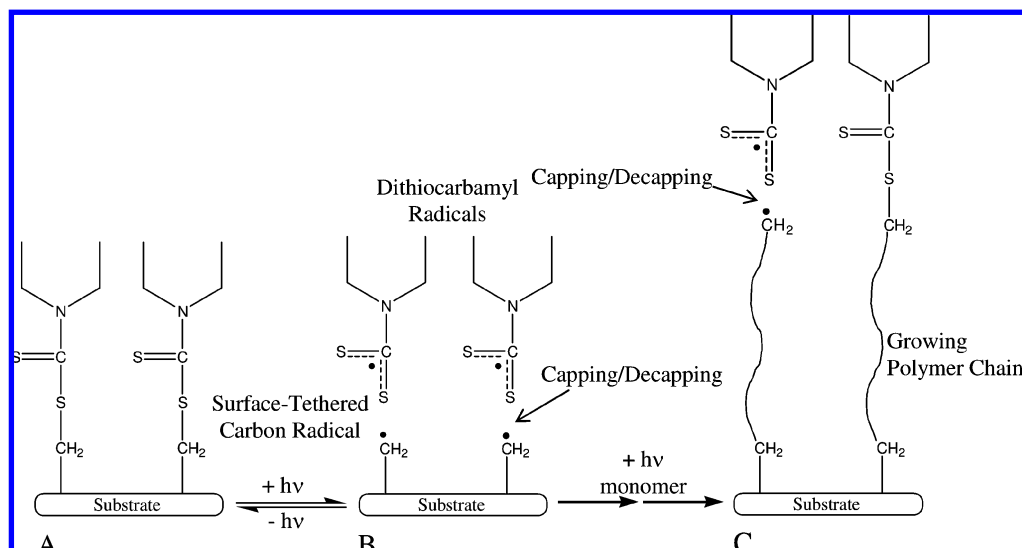


Figure 2. Living radical photopolymerization using DTC species provides a convenient means of controlling surface properties and studying their effects on, for example, the antibacterial activity of polymerizable antibiotics. (A,B) Dithiocarbamyl species are cleaved by UV light to form surface-attached carbon radicals as shown in panel B. (C) When monomer is included in the system, polymer chains grow from the surface. They are continually terminated and reinitiated (“capping/decapping”) in the presence of UV light, creating a dynamic equilibrium which, in principle, decreases polydispersity of polymer chains and reduces undesirable chain transfer and chain termination events. Surface-grafted polymer chains lengthen as polymerization time is increased.

this leads to cooperative ligand binding by increasing the effective antibiotic concentration in the vicinity of other ligands.³³ A wide literature exists describing the glycopeptides, their mechanism of action, and combinatorial approaches to increasing their potency,^{33–47} potentially facilitating the cogent design of new polymerizable analogs. Of note, Arimoto et al. first described vancomycin-based norbornene monomers synthesized through a ring-opening metathesis polymerization with a Grubb’s ruthenium catalyst.^{30,31} It was demonstrated that a polymer mixture containing 2 to ca. 15-mers was capable of restoring antibacterial activity against vancomycin resistant enterococcus (VRE). However, structural analysis of monomers and polymers was limited.

Beyond understanding the influence of the synthetic functionalization chemistry on vancomycin activity, a second important aspect requires characterization of bactericidal activity of copolymers formed from these polymerized molecules. Surface-mediated polymerization through an iniferter-based chemistry is an attractive option for biomaterial surface modification. Iniferter surface techniques provide a facile means to modify materials with desired functional groups.^{48–52} Many iniferters are dithiocarbamate (DTC) derivatives that, upon homolytic bond cleavage, yield a reactive carbon radical and a dithiocarbamyl radical. The carbon radical readily reacts with vinyl monomers (e.g., acrylates), whereas the dithiocarbamyl radical reacts only minimally.^{53–55} However, the dithiocarbamyl radical does reversibly terminate growing polymer chains (“capping/decapping”) and, depending on reaction conditions, leads to controlled free-radical polymerization (Figure 2).^{48,51,53,56}

Recently, we reported the synthesis of a polymerizable, poly(ethylene glycol)(PEG)-acrylate derivative of vancomycin. This species was successfully polymerized to an orthopedic titanium alloy to form a bactericidal surface.²⁹ However, no systematic evaluation of monomer structure was conducted, particularly in relation to biochemical function. We hypothesize that both the length of the PEG spacer and the site of vancomycin functionalization will affect solution-based and surface-based antibacterial activity through several possible mechanisms. These include interference with specific hydrogen

bonds important for binding D-Ala-D-Ala, as well as blocking of vancomycin dimer formation. Here, we also investigate the effects of monomer composition (relative concentration of the polymerizable vancomycin analogue to the comonomer) and monomer structure (PEGylated versus non-PEGylated monomer and also the site of vancomycin modification) on surface-based antibacterial activity using bioassays with *Staphylococcus epidermidis* bacteria.

Materials and Methods

Synthesis of PEG-Acrylate and Acrylamide Vancomycin Derivatives. Vancomycin-PEG(X)-acrylate [VPA(X)] derivatives (where X = the number average molecular weight of the PEG chain, either 3400 or 5000) were synthesized with slight modification from a previous protocol.²⁹ Briefly, vancomycin hydrochloride (Sigma Aldrich, St. Louis, MO) was reacted with *N*-hydroxysuccinimide-PEG(X)-acrylate [NHS-PEG(X)-acrylate] (Nektar Therapeutics, San Carlos, CA) in a 4:1 ratio for 24 h in anhydrous dimethyl sulfoxide (DMSO) at room temperature (Figure 3).

Vancomycin-acrylamide derivatives were synthesized (Figure 4) by two different procedures. When V₃-modified vancomycin was desired, vancomycin hydrochloride was dissolved in deionized H₂O and the pH was adjusted to 10.5 by addition of NaOH. The solution was then frozen and lyophilized. When dry, the lyophilized powder was dissolved in anhydrous DMSO. Separately, equal volumes of *N,N'*-diisopropylcarbodiimide (DIC) (Sigma Aldrich, St. Louis, MO) and acrylic acid (Fisher Scientific, Pittsburgh, PA) were reacted in anhydrous DMSO for ca. 20 min. Following formation of a reactive *O*-acylisourea intermediate, this solution was added to the previously prepared vancomycin solution and vortexed for 3 h at room temperature to give vancomycin acrylamide derivatives (V₃ and X₁ functionalized). Conditions were chosen to provide for a maximum 2:1 ratio of *O*-acylisourea intermediate to vancomycin. The reaction was terminated by addition of H₂O. When X₁-modified vancomycin was desired, an analogous procedure was followed without the initial pH adjustment.

Liquid Chromatographic Product Purification. To remove DMSO and residual vancomycin, VPA(X) derivatives were purified by 24 h dialysis against 1 M NaCl followed by 24 h against deionized H₂O using 3,500 molecular weight cutoff dialysis cassettes. Dialysis was

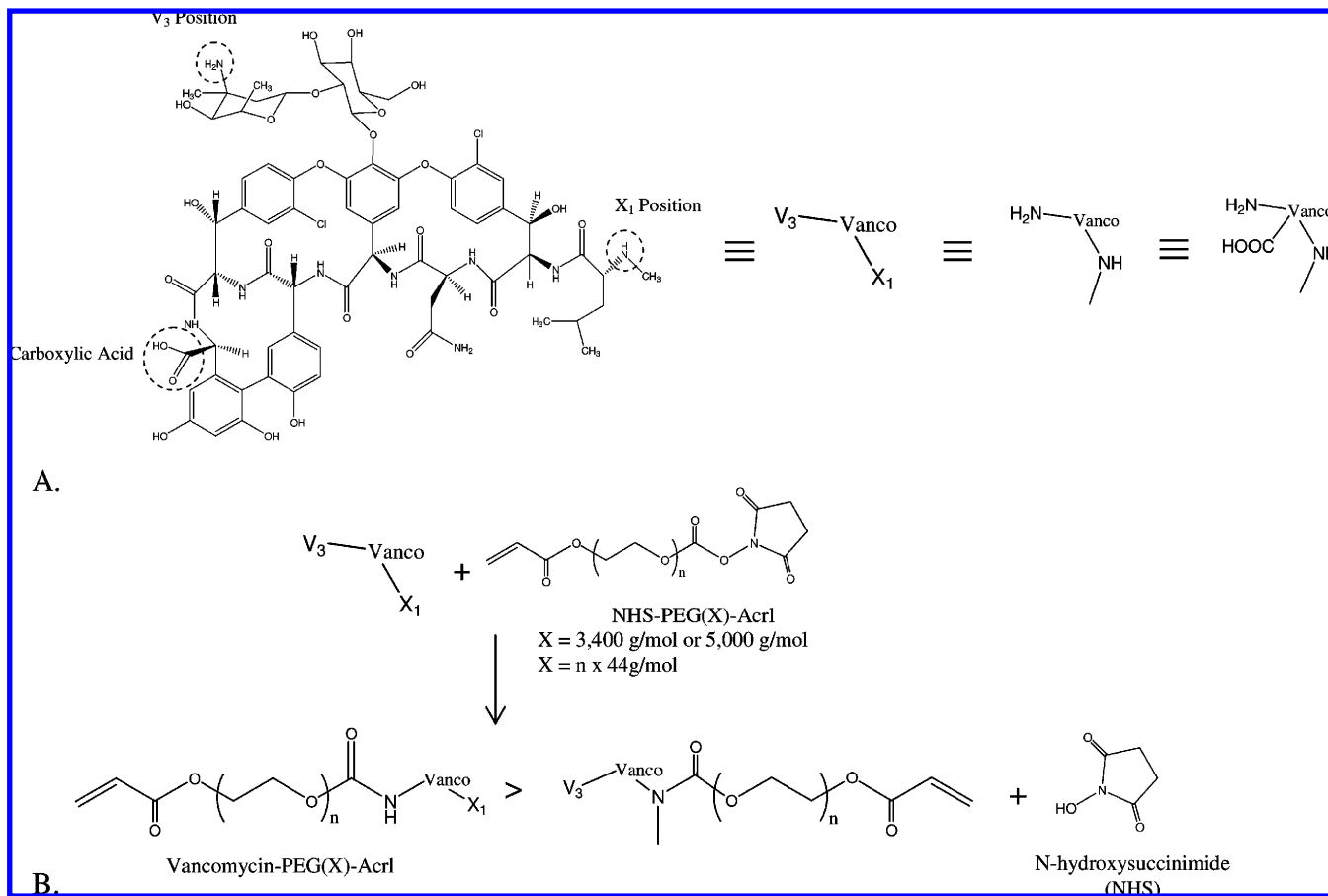


Figure 3. (A) Vancomycin is typically modified at one of three sites (dashed circles). The glycosidic primary amine is termed the V_3 position, and the nonamide secondary amine is termed the X_1 position. Three structural abbreviations are shown and will be used in subsequent figures. (B) VPA(X) species were synthesized using NHS-PEG(X)-acrylate, a reactive ester that favors reaction with primary amines over secondary amines.

followed by $0.2 \mu\text{m}$ syringe filtration and size exclusion chromatography on a Sephadex G-50F (Amersham Biosciences, Uppsala, Sweden) column with dimensions $33 \text{ cm} \times 2.5 \text{ cm}$ (length \times i.d.) and deionized H_2O as the mobile phase. Products were recovered by spectrophotometric analysis of column breakthrough at 220 nm using a Lambda 40 UV/vis spectrophotometer (PerkinElmer Instruments, Wellesley, MA). Appropriate fractions were collected, frozen, and lyophilized before further analysis.

Vancomycin acrylamide derivatives were purified by high-pressure liquid chromatography (HPLC) using a SymmetryPrep C18 reverse-phase column of dimensions $19 \times 300 \text{ mm}$ on a DeltaPrep 4 HPLC system (Waters Corporation, Milford, MA). All solvents were HPLC-grade with 0.1% (v/v) trifluoroacetic acid to limit product aggregation. Following the synthetic procedures described above, crude product was loaded onto the column and run with an appropriate acetonitrile/ H_2O gradient. Product peaks were collected by dual-wavelength spectrophotometric detection at 220 nm and 280 nm. Recovered products were frozen, lyophilized, and examined for purity on a Symmetry analytical reverse-phase C18 column of dimensions $4.6 \times 150 \text{ mm}$ again using an appropriate solvent gradient.

Matrix-Assisted Laser Desorption Ionization Mass Spectrometry (MALDI-MS). MALDI-MS was used to confirm product isolation following liquid chromatography. The matrix solution for all samples was saturated 2-(4-hydroxyphenylazo)benzoic acid (Fluka, St. Louis, MO) in 50:50 spectrophotometric-grade methanol and HPLC-grade water. A Voyager-DE STR BioSpectrometry Workstation mass spectrometer (PerSpective Biosystems, Waltham, MA) was used for data acquisition.

Nuclear Magnetic Resonance (NMR) Spectroscopy. 500 MHz ^1H NMR spectra were obtained for all polymerizable antibiotic monomers

in either DMSO-d_6 or D_2O on a Varian Inova-500 spectrometer (Varian, Inc., Palo Alto, CA) at product concentrations of ca. 20 mg/mL. Two-dimensional (2D) NMR experiments were conducted with vancomycin acrylamide species to determine the site of acrylamide functionalization. These experiments included gradient-selected correlation spectroscopy (gCOSY), heteronuclear single quantum coherence (gHSQC) spectroscopy, and heteronuclear multibond correlation (gHMBC) spectroscopy.

Minimum Inhibitory Concentration (MIC) and Minimum Bactericidal Concentration (MBC). MIC and MBC values for each monomer were determined in at least triplicate by the broth dilution method as described elsewhere.²⁹ The MIC was defined as the lowest antibiotic concentration at which no turbidity was observed in growth suspensions. The MBC was taken to be the lowest monomer concentration at which 99.9% of the initial bacterial inoculum was killed.

In the case of the VPA(X) species, two computational corrections were made to the experimentally determined MIC values to account for: (1) unfunctionalized PEG(X)-acrylate not removed by size exclusion chromatography; and (2) a small amount of residual vancomycin (ca. 0.4 wt % of the final product). Residual vancomycin was determined by HPLC with peak integrations by Simpson's Rule.⁵⁷ Residual PEG(X)-acrylate was estimated by ^1H NMR integrations. The PEG(X)-acrylate correction was made by multiplying the total number of moles of MIC material [moles PEG(X)-acrylate plus moles VPA(X)] by the mole fraction of VPA(X) (decimal % product by NMR). It is assumed that PEG(X)-acrylate has computationally insignificant antibacterial activity, which is consistent with previous studies showing PEG(400) to have a MIC of ca. $4000 \mu\text{g/mL}$ against *S. aureus*⁵⁸ and p-hydroxyphenyl acrylate to have a MIC of ca. $625 \mu\text{g/mL}$ against *S. epidermidis*.⁵⁹ Moreover, potential probiotic effects of oligoethylene oxide should be of negligible concern as the only known aerobic, gram-

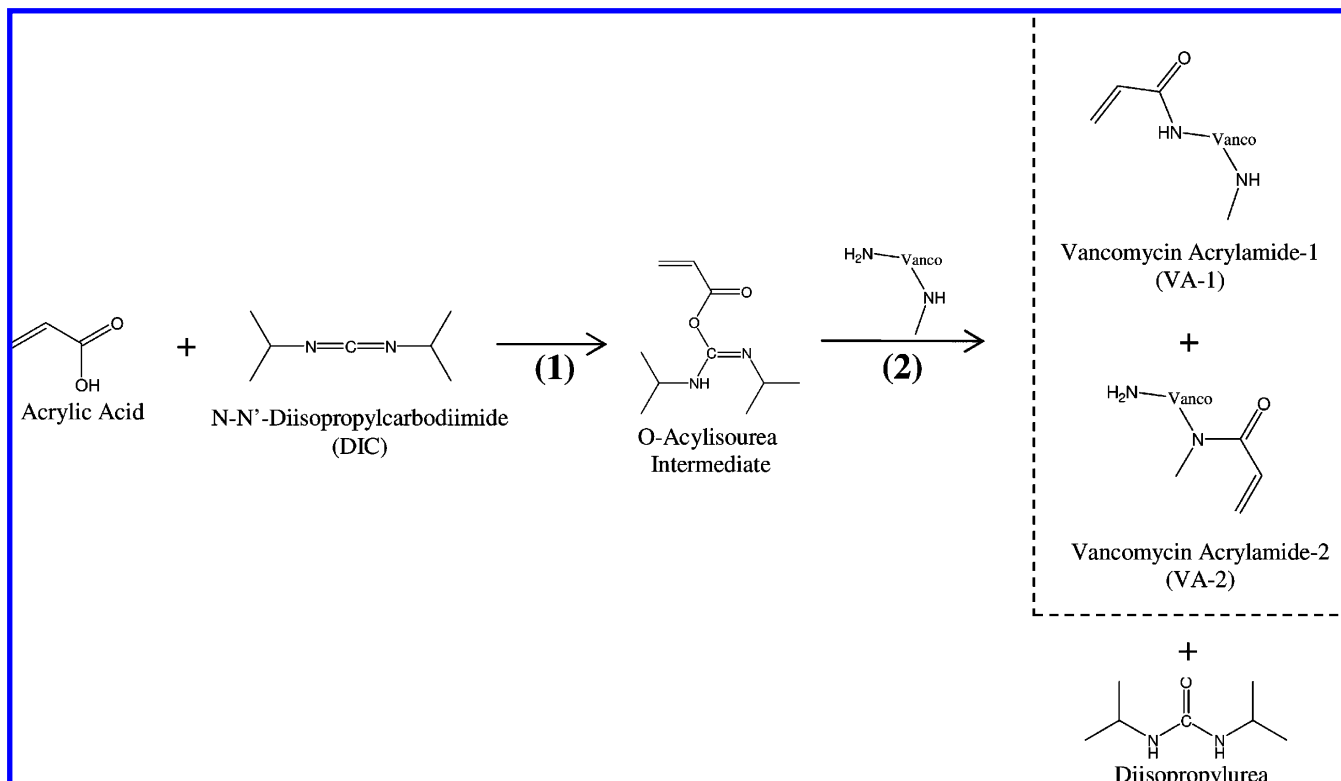


Figure 4. Vancomycin–acrylamide species were synthesized using carbodiimide chemistry. To minimize side reactions, the reactants for (1) are allowed to prereact before vancomycin is added. This reduces activation of the vancomycin carboxylic acid by DIC and subsequent side reactions. DIC chemistries are preferred over NHS esters for reactions at secondary amines and, thus, provided a means for synthesis of both VA-1 and VA-2. Although not illustrated here, it is possible to obtain polymerizable vancomycin dimers using DIC chemistries, which may be useful in light of the importance of dimers in glycopeptide antibiotic function.

positive, PEG-degrading bacteria cover some species in the genera *Rhodococcus*, *Williamsia*, *Bacillus*, *Mycobacterium*, and *Pseudonocadia*.⁶⁰ Nevertheless, PEG(X)-acrylate does lead to a systematic, gravimetric error in MIC determinations. Following PEG(X)-acrylate correction, the result was adjusted for residual vancomycin according to

$$\frac{C_{\text{vanco}}}{\text{MIC}_{\text{vanco}}} + \frac{C_{\text{VPA(X)}}}{\text{MIC}_{\text{VPA(X)}}} = 1 \quad (1)$$

where C_{vanco} ($\mu\text{mol/L}$) is the concentration of residual vancomycin in the experiment, $\text{MIC}_{\text{vanco}}$ ($\mu\text{mol/L}$) is the previously determined MIC value for vancomycin, $C_{\text{VPA(X)}}$ ($\mu\text{mol/L}$) is the true concentration of VPA(X) necessary to inhibit bacterial growth in the presence of contaminating vancomycin, and $\text{MIC}_{\text{VPA(X)}}$ ($\mu\text{mol/L}$) is the MIC value for VPA(X). This expression simply assumes that the effects of vancomycin and VPA(X) are additive in the absence of synergistic behavior. However, what is measured in the experiment is the total amount of material added to the culture tube:

$$C_{\text{VPA(X)}}^{\text{obsd}} = C_{\text{VPA(X)}} + C_{\text{vanco}} \quad (2)$$

Thus, after combination and rearrangement,

$$\text{MIC}_{\text{VPA(X)}} = (C_{\text{VPA(X)}}^{\text{obsd}} - C_{\text{vanco}}) \cdot \left(1 - \frac{C_{\text{vanco}}}{\text{MIC}_{\text{vanco}}}\right)^{-1} \quad (3)$$

This correction is necessary because $\text{MIC}_{\text{vanco}}$ tends to be a small value for most *Staphylococcus* species. MBC values were corrected in an analogous fashion. Error estimates were computed using standard

propagation of uncertainty equations described elsewhere⁶¹ to ensure that the most conservative (largest) error estimates were calculated. For these propagation of uncertainty calculations, the following underlying errors were assumed: 10% error in NMR integrations (a typical maximum error estimate); 10% error in residual vancomycin estimates (estimated maximum HPLC error); 10% error in the vancomycin MIC value.

Molecular Dynamics Simulations. Molecular modeling of polymerizable vancomycin derivatives was conducted using the molecular mechanics feature of CS Chem3D Pro v. 7.0 (CambridgeSoft, Cambridge, MA) with the intent of exploring conformational energy minima. Structures were imported from CS ChemDraw v. 7.0 (CambridgeSoft, Cambridge, MA), and the energy minimization routine was run with a root-mean-square (rms) gradient of 0.100. Molecular dynamics simulations were then run at 330 K (37 °C) with a step interval of 2.0 fs, a frame interval of 10 fs, and a heating rate of either 0.0 or 1.0 kcal/atom/ps. Simulations were stopped after 10 000 steps. Specific atomic separation distances were followed (e.g., between the acrylamide carbonyl of VA-2 and a local amide hydrogen known to hydrogen-bond with bacterial D-Ala-D-Ala), and the energy minimization routine was performed beginning at frames of interest to explore various local energy minima.

DTC Substrate Preparation. DTC grafting substrates were prepared from monomer formulations consisting of aromatic urethane diacrylate (UDA) (Cytec-Surface Specialties, Smyrna, GA) and triethylene glycol diacrylate (TEGDA) (Sartomer, Exton, PA) mixed with 1 wt % tetraethylthiuram disulfide (TED) (Sigma-Aldrich, St. Louis, MO) and 1.5 wt % 2,2-dimethoxy-2-phenylacetophenone (DMPA) (Ciba-Geigy, Hawthorne, NY) photoinitiator as described elsewhere.⁶² The substrate was photopolymerized by exposure to a 45 mW/cm² intensity, collimated, broad-range, UV light (Hg arc-lamp centered at 365 nm) for 900 s using a Hybralign Series 200 mask alignment system (Oriental Instruments, Stratford, CT). These exposure conditions yield a poly-

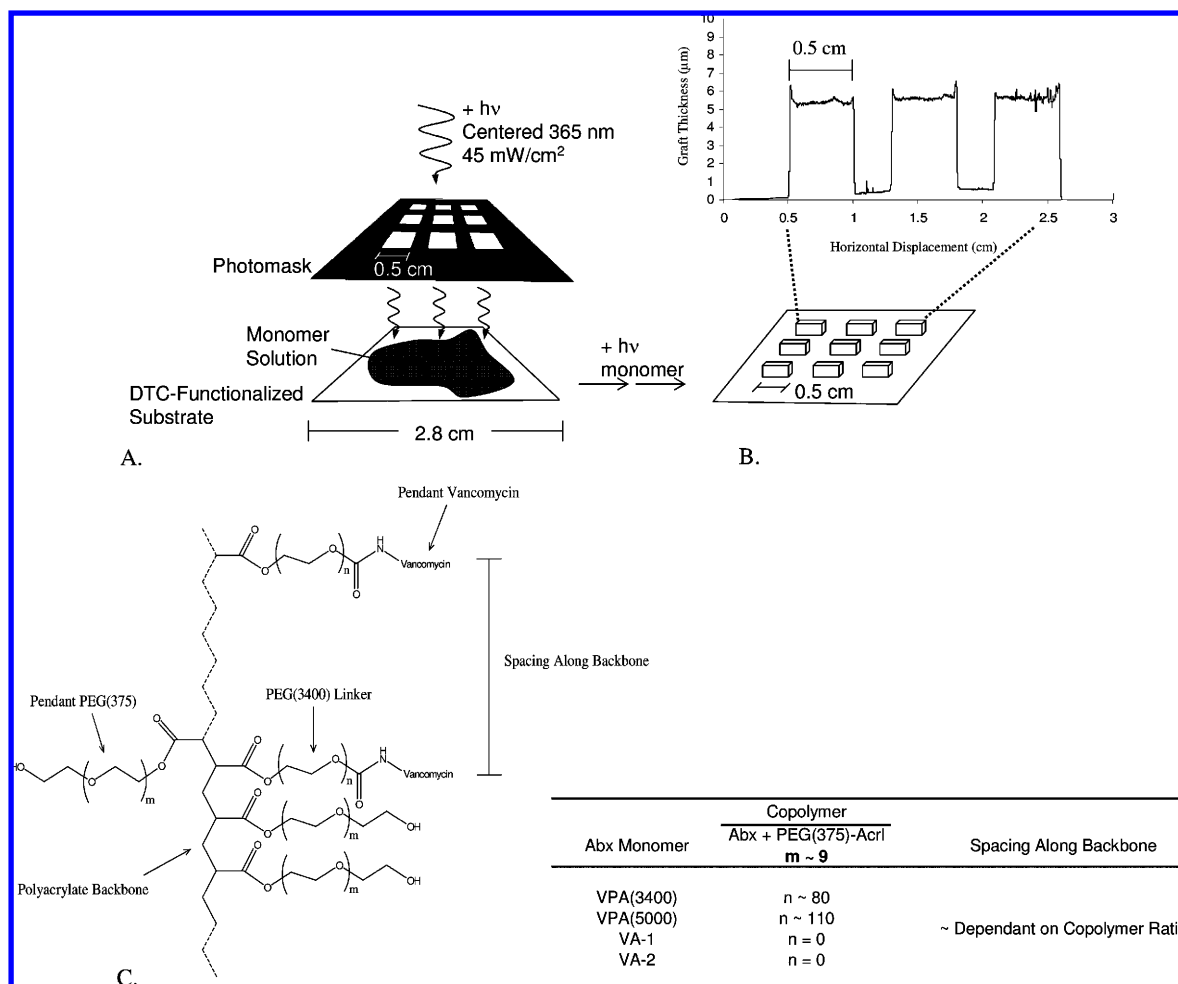


Figure 5. (A) Photolithographic techniques were used to pattern antibacterial polymer on a DTC-functionalized surface. UV light passes through the transparent regions of the photomask (squares) and polymerizes the underlying monomer solution containing polymerizable antibiotic and an appropriate comonomer. (B) Polymer squares are grafted from the surface and are used for testing polymer antibacterial activity. The inset shows a profilometry trace through three grafted squares. Grafts on the order of $5 \mu\text{m}$ thickness were used throughout the experiments described here. This is about 5 times the diameter of a *S. epidermidis* organism. (C) Shown is the expected dominant polymer structure when a VPA(X) monomer is copolymerized with PEG(375)-acrylate. A polyacrylate backbone is formed by chain polymerization. Pendant to the backbone are both PEG(375) functionalities ($m \sim 9$) and vancomycin-PEG(X) groups ($n \sim X/44$, where 44 g/mol is the molecular weight of an ethylene glycol repeat). To a first approximation, the spacing between vancomycin groups ("spacing along backbone") is given by the ratio of VPA(X):PEG(375)-acrylate in the monomer solution.

meric network with over 90% double bond conversion when monitoring the acrylate double bond absorbance peak by near-IR spectroscopy.⁶² Once polymerized, substrate samples were washed in copious amounts of methanol to remove any unreacted species prior to the photografting procedure.

Photografting of VPA(X) and Vancomycin Acrylamides. Polymerizable vancomycin derivatives were covalently photografted from the DTC-functionalized substrate surfaces using iniferter-based photopolymerization chemistry. Grafting solutions were created by dissolving VPA(3400) to a concentration of 200 mg/mL (true concentration) in Ar-purged DMSO then serially diluting with PEG(375)-acrylate/DMSO solutions of desired composition. Final graft solutions were targeted to desired molar ratios of VPA(3400)/PEG(375)-acrylate (e.g., 1:50, 1:100, etc.). VPA(5000) grafting solutions were made in an analogous fashion. Surfaces were modified by photopolymerization of 40 μL of a comonomer solution initiated by exposure to the light source described above for 300 s. A patterned region (3×3 array of squares having dimensions $0.5 \text{ cm} \times 0.5 \text{ cm} \times \sim 5 \mu\text{m}$ height) of grafted antibiotic/comonomer was formed using photolithographic techniques also described in part elsewhere (Figure 5A,B).⁶² The resulting polymers have a polyacrylate backbone with pendant ethylene glycol units and pendant vancomycin or PEG(X)-vancomycin (Figure 5C). Following polymerization, surfaces were washed with copious amounts of ethanol.

An extended elution series consisting of ethanol, sodium chloride, and deionized water soaks was employed for ca. 24 h to remove any entrapped or aggregated antibiotic monomer. Surface grafts were then characterized by profilometry using a Dektak 6 M Stylus Profilometer (Veeco Instruments, Inc., Woodbury, NY) to determine graft thickness. Vancomycin acrylamide graft polymerizations were conducted in an analogous fashion.

Surface Antibacterial Assays. Using aseptic technique, grafted squares (elements of the aforementioned 3×3 arrays) of antibacterial copolymers were isolated with a hydrophobic PAP pen and exposed to a 40 μL aliquot of brain heart infusion (BHI) media containing 1×10^4 colony forming units (CFU)/mL *S. epidermidis* ATCC 12228 (MicroBiologics, Inc., St. Cloud, MN) for 20 h at 37 °C. This surface challenge time was chosen to simulate the initial bacterial seeding as might occur following the implantation of orthopedic hardware and to demonstrate bactericidal activity. It is acknowledged that, under some in vivo conditions, surfaces will be challenged for longer periods of time and challenged repeatedly. Following incubation, the suspensions were sampled, serially diluted with sterile, deionized water, and plated on trypticase soy agar with 5% sheep blood (Becton, Dickinson, and Co., Sparks, MD) for CFU counts. Various surface densities of polymerizable antibiotic were assayed for activity. Activity was reported in terms of log reduction relative to nonantibiotic control surfaces.

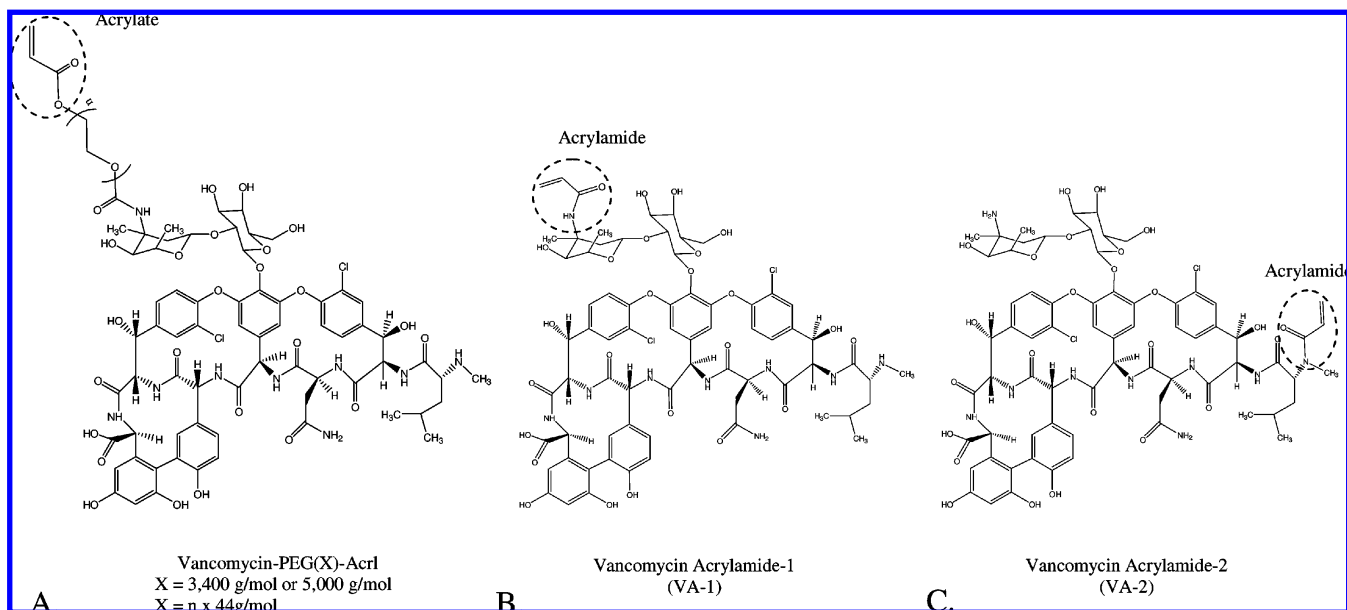


Figure 6. (A) PEG-acrylate derivatives of vancomycin potentially offer advantages related to PEGylation while at the same time allow for facile polymerization to biomaterial constructs through the acrylate group. Here, we present two such species, one having a 3400 molecular weight PEG spacer and the other having a 5000 molecular weight spacer. The molecular weight of an ethylene oxide repeat is 44 g/mol. (B) Vancomycin acrylamide derivatives are structurally similar but lack the PEG spacer. VA-1 is modified at the glycosidic primary amine of vancomycin. (C) VA-2 is modified at the sole nonamide secondary amine.

Elution controls were employed to differentiate surface-based activity from simple release of antibiotic moiety (see below).

Elution Controls. Elution controls were conducted using bioassays similar to those described previously²⁹ to verify that no detectable vancomycin was released from the grafts over a time frame commensurate with the surface antibacterial assays. For each grafted 3×3 array of test squares, at least one control square was exposed to a sterile $40 \mu\text{L}$ aliquot of BHI media that was coincubated with the other bacteria-exposed squares. Following incubation, $10 \mu\text{L}$ of this media were collected, frozen, lyophilized, then inoculated with $10 \mu\text{L}$ deionized water containing 1×10^4 CFU/mL of the test organism. The solution was incubated for 20 h at 37°C , and a visibly positive culture was taken as indicative of undetectable antibiotic elution.

Statistical Analysis. All statistical calculations were performed using Minitab15 statistical software (Minitab, Inc., State College, PA). MIC and MBC data are most properly compared using a nonparametric method such as the Mann–Whitney test, which makes no assumption about an underlying distribution and is appropriate for discrete data. However, our raw VPA(X) data required a propagation of uncertainty calculation following adjustment for residual PEG(X)-acrylate and residual vancomycin (see eqs 1–3). Thus, statistical comparisons of MIC and MBC parameters were calculated by both the Mann–Whitney test using raw data and the student *t* test using propagation of uncertainty information. In general, both methods were in good agreement with a chosen $\alpha = 0.1$. Reported *P* values are the more conservative (larger) for a given comparison.

Results and Discussion

Implantable devices have become common in most fields of medicine, and various design issues including tissue integration, immunogenicity, and material degradation must be considered. Regardless of implant type, infections secondary to microbial colonization remain a significant clinical concern. Thus, there has been an increased interest in developing new materials for either delivering antibiotics locally^{63–67} or for surface-modifying biomaterials with antibacterial functionalities.^{29,68–70} Polymerizable derivatives of traditional antibiotics offer potential for controlled biomaterial surface modification. Here, we describe

the synthesis and characterization of several monomeric vancomycin derivatives and relate MIC data to structural characteristics of various monomers through both 2D NMR techniques and molecular dynamics simulations. We conclude with an iniferter-based platform for ascertaining structure–function biochemical relationships of polymerized constructs with the ultimate goal of facilitating the trenchant design of polymerizable, surface-active antimicrobials and other pharmaceutical species.

Synthesis and Characterization of Monomers. Two vancomycin–PEG-acrylate species and two vancomycin acrylamide species (Figure 6) were synthesized.

The PEG-acrylate derivatives differ in the molecular weight of the PEG chain (number average molecular weight ~ 3400 g/mol versus ~ 5000 g/mol), and the acrylamides differ at the site of vancomycin modification (glycosidic primary amine at the V_3 position versus the lone, nonamide secondary amine at the X_1 position) (Figure 3A). These species are in some sense similar to the norbornene derivatives described by Arimoto et al.,^{30,31} however, the compounds described there were modified solely at the V_3 position without PEG linkers. Moreover, the subsequent polymerization scheme relied upon a ruthenium Grubb's catalyst and required approximately 1.5 days to yield useful polymeric material, whereas the current approach achieves bactericidal polymers on the order of minutes.

Consistent with our VPA(X) synthesis protocol, size exclusion liquid chromatography results (not shown) demonstrated two peaks for a given VPA(X) type: a lead peak at ca. 25 min containing high molecular weight compounds that eluted with the void volume (confirmed with blue dextran); and a product peak at ca. 30 min for VPA(5000) or ca. 35 min for VPA(3400). The absence of a third peak suggests that the dialysis procedure removed most residual vancomycin and small-molecule species. The high molecular weight byproducts (lead peak) in our synthesis scheme likely represent products formed by autopolymerization of monomer based on ^1H NMR results (not shown). In the case of VPA(3400), MALDI-MS indicated that the

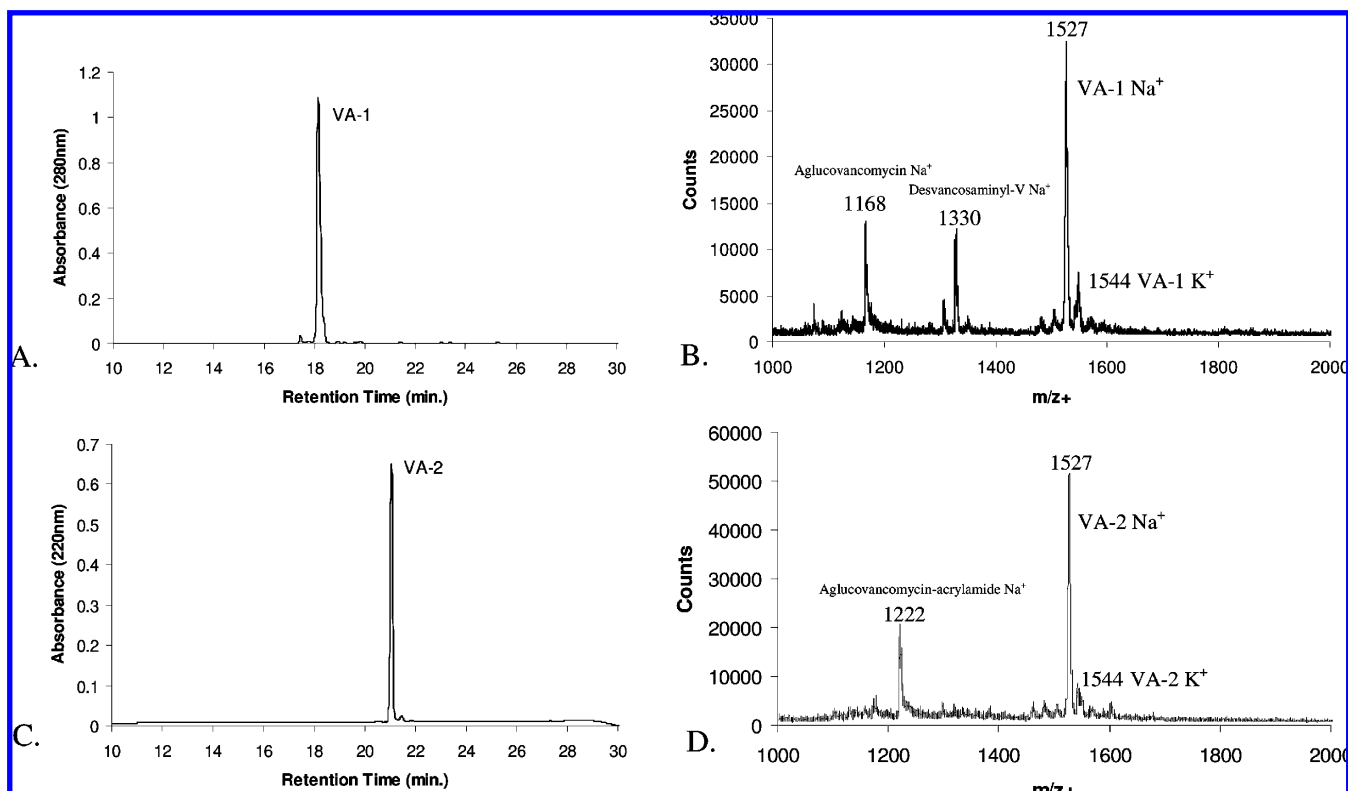


Figure 7. (A,C) C18 analytical reverse phase HPLC with VA-1 and VA-2 showed that the products were clean (>95%). (B,D) MALDI-MS showed the expected Na^+ peaks in addition to low-level contamination from various vancomycin-type species such as aglucovancomycin, desvancosaminylvancomycin, and aglucovancomycin acrylamide.

Table 1. MALDI-MS, Liquid Chromatography, and ^1H NMR Results for the Four Polymerizable Vancomycin Derivatives

species	m/z^+ (calcd, Na^+)	m/z^+ (obsd, Na^+)	HPLC rt (min.)	gel filtration rt (min.)	solvent	NMR integrations relative to a vinyl H			
						methyl H's (calcd)	methyl H's (obsd)	methyl (obsd)/ methyl (calcd)	% product by NMR
vancomycin	1473.3	1472.7	16.5	variable (aggregation effects)	DMSO	6.0	6.0	1.00	100%
VPA(3400)	ca. 4900	ca. 4800	35		D_2O	6.0	3.7	0.62	62%
VPA(5000)	ca. 6500	ca. 6500	30		D_2O	6.0	3.3	0.55	55%
VA-1	1527.3	1526.9	18.2		DMSO	6.0	6.0	1.00	100%
VA-2	1527.3	1526.8	21.1		DMSO + D_2O	6.0	5.6	0.93	93%

product gel filtration peak contained a polymeric species of ca. 3500 g/mol molecular weight [residual PEG(3400)-acrylate] and a polymeric species of ca. 4800 g/mol molecular weight [VPA(3400)]. A repetitive 44 g/mol spacing was noted throughout the molecular weight distributions, which is characteristic of PEG polymers: the polydispersity index (PDI) of NHS-PEG(3400)-acrylate used in the synthesis was ca. 1.03. A similar result was obtained with VPA(5000), but the central molecular weights were shifted to 5000 g/mol and 6500 g/mol; the PDI of NHS-PEG(5000)-acrylate used in the synthesis was ca. 1.05.

Analytical HPLC results obtained following the vancomycin acrylamide synthesis protocol(s) showed that each of the recovered materials eluted as a dominant, symmetric peak with only low-level contamination (estimated at >95% purity). However, the retention times differed by ca. 3 min. MALDI-MS results indicated that these two peaks were of the same molecular weight (Figure 7B,D), which suggested that one species was VA-1 and the other VA-2. MALDI-MS also showed that purified VA-1 contained some residual material attributed to aglucovancomycin (both sugars removed) (Figure 7B) and desvancosaminylvancomycin (terminal sugar removed), which is consistent with species known to be present in commercially available vancomycin preparations.³⁸ The VA-2 peak contained

residual material attributed to aglucovancomycin acrylamide (Figure 7D).

^1H NMR characterization of the VPA(X) species demonstrated the expected functionalities. Using VPA(3400) as an example, chemical shifts were as follows: vinyl hydrogens from the acrylate ($\delta = 6.0$, 1H, doublet; $\delta = 6.2$, 1H, multiplet; $\delta = 6.4$, 2.7H, doublet, convoluted with aromatic Hs); PEG hydrogens ($\delta = 3.4 - 3.8$); aromatic hydrogens from vancomycin ($\delta = 6.4 - 7.8$); and methyl hydrogens from vancomycin ($\delta = 0.9$, 3.7H, doublet). Six methyl hydrogens are expected for pure VPA(X), indicating that the recovered material was approximately 60% VPA(3400) and 40% PEG(3400)-acrylate. The acrylamide derivatives gave similar spectra without the PEG peak. The pertinent vinyl and methyl integrations and comparisons to calculated values are presented below (Table 1).

To determine the site of acrylamide functionalization on vancomycin acrylamide derivatives, 2D NMR experiments were conducted. gCOSY spectra for VA-2 are shown below (Figure 8A-B). Off diagonal peaks represent correlations between hydrogens on adjacent carbons, while the peaks on the diagonal are representative of the corresponding ^1H shifts. The gCOSY spectra revealed the presence of an acrylamide functionality.

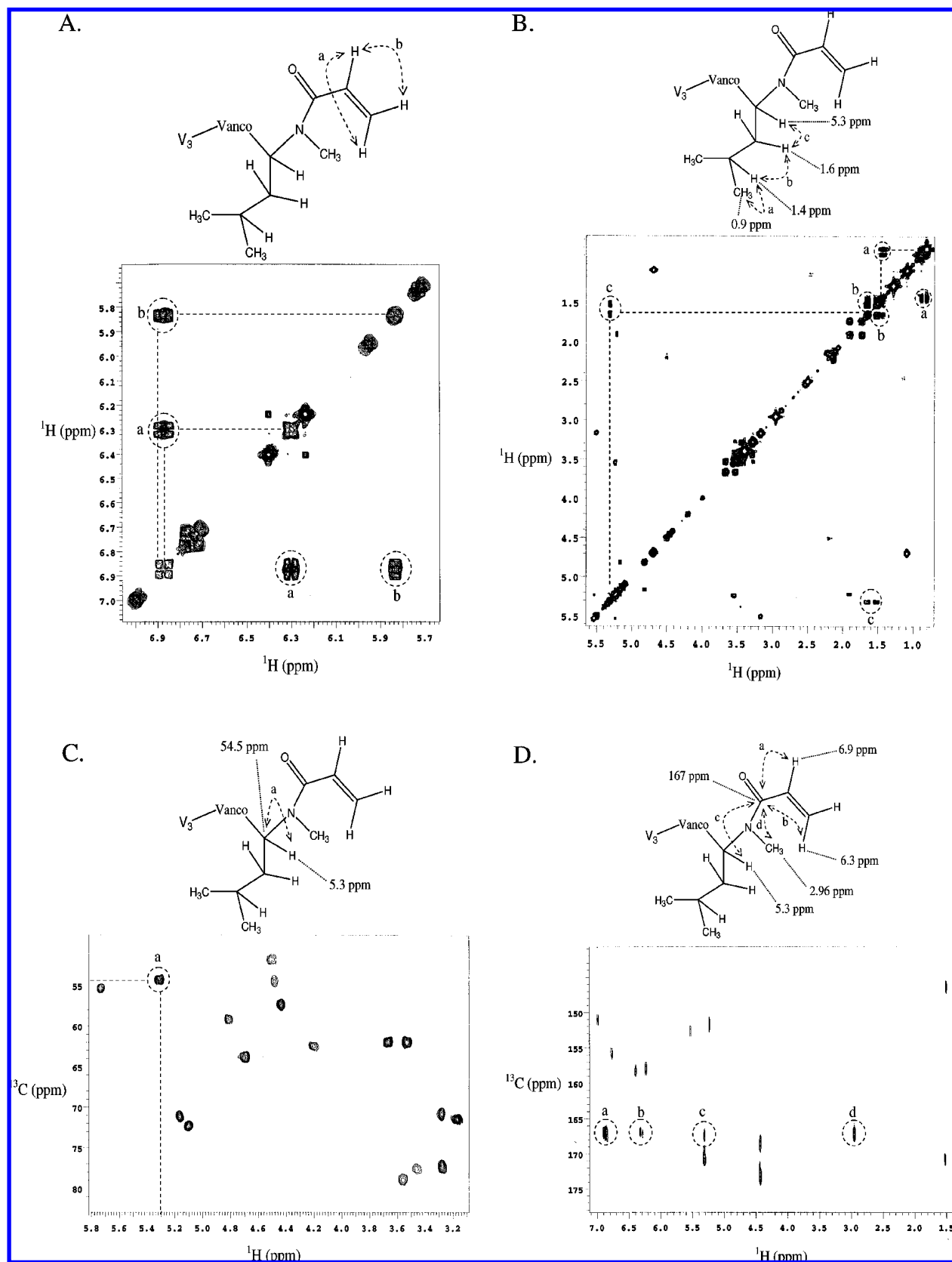


Figure 8. (A) gCOSY spectrum of VA-2. Correlations between vinyl protons are shown (dashed circles, arrows, and lines). (B) A more complete gCOSY spectrum of VA-2 allowed for assignment of ^1H chemical shifts along part of the aliphatic backbone of the molecule. Three correlations are shown (dashed circles and lines). (C) gHSQC experiments which establish correlations between ^{13}C and ^1H nuclei were used to assign pertinent ^{13}C shifts once the ^1H shifts were known. (D) A gHMBC experiment was used to establish correlations between ^{13}C nuclei and ^1H nuclei up to three bonds distant. Here, four important correlations are noted (dashed circles) that place the N-CH₃ group along the previously defined molecular backbone as well as establish its vicinity to the carbonyl of the acrylamide group. These correlations definitively place the acrylamide group at the vancomycin X₁ position.

The locations of the acrylamide was determined using gCOSY in conjunction with gHSQC and gHMBC NMR spectroscopy. A complete gCOSY and a gHSQC spectra are shown below for VA-2 (Figure 8B,C). gCOSY analysis allowed for the determination of the chemical shifts of hydrogens along the vancomycin molecule starting from the known methyl hydrogen shift at 0.9 ppm. The relevant ^1H shifts are illustrated (Figure 8B). gHSQC establishes correlations between carbon atoms and their attached hydrogens. Thus, gHSQC was used to identify the ^{13}C shift (54.5 ppm) of the tertiary carbon directly bound to the vancomycin X_1 secondary amine (Figure 8C).

gHMBC, optimized for correlations between carbons and hydrogens three-bond distance, was used to establish the ^1H shift of the $\text{N}-\text{CH}_3$ hydrogens at the X_1 position as well as to correlate the carbonyl of the acrylamide to the $\text{N}-\text{CH}_3$ hydrogens, definitively establishing that VA-2 is the X_1 -modified vancomycin acrylamide derivative (Figure 8D). A similar analysis (not shown) with VA-1, established that VA-1 was the V_3 -modified acrylamide species.

Our VPA(X) synthesis procedures made use of *N*-hydroxysuccinimidyl ester starting reagents of a type that readily reacts with primary amines and less readily with secondary amines and alcohols. The esters formed by the reaction with alcohols are unstable and readily hydrolyze.⁷¹ Thus, our VPA(X) species should be primarily of the V_3 -modified type, which places the PEG linker opposite the binding pocket of the vancomycin molecule. ^1H NMR confirmed that our synthesized VPA(X) molecules did have both PEG-acrylate and vancomycin functional characteristics, and MALDI-MS results suggest that we were able to recover singly functionalized VPA(X) using a Sephadex G-50F size exclusion column. Likewise, the synthetic approach used to construct vancomycin acrylamide monomers made use of well-established chemistries of the carbodiimide variety.⁷¹ The main drawback of these chemistries is the relatively high reactivity of *O*-acylisourea intermediates and the possibility of side reactions. However, some control was afforded through optimization of reactant stoichiometry and reaction times, and we were able to isolate the desired vancomycin acrylamide derivatives (VA-1 and VA-2) as confirmed by analytical HPLC, MALDI-MS, and various NMR techniques. In conjunction with proper HPLC protocols, carbodiimide chemistry offers an opportunity to isolate several interesting and potentially bioactive species. Polymerizable vancomycin dimers, for example, might offer increased potency with respect to the species presented here in light of other studies with multivalent antibiotics.^{39,43,45}

Molecular Dynamics Simulations. Molecular dynamics simulations with VA-2 at 37 °C and no heat input indicated that the acrylamide carbonyl oxygen assumes a local energy minimum when placed within 1.9–2.1 Å of an amide hydrogen located on the vancomycin backbone. This hydrogen normally plays a role in H-bonding bacterial D-Ala-D-Ala, suggesting that adding an acrylamide to the vancomycin X_1 position competitively blocks this interaction (Figure 9A). When heat was added to the system at a rate of 1.0 kcal/atom/ps, adequate energy was afforded for the molecule to escape this conformation. However, the ca. 2.0 Å separation still remained a favorable conformational energy minimum.

Molecular dynamics simulations with VPA(X) species did not point to a single molecular conformation that was responsible for decreased activity. It was found that with a long PEG linker (ca. 80 repeat units were used in simulations), there existed almost endless energetically favorable geometries between the vancomycin moiety and the attached PEG chain. Twisted, coiled,

and linear structures were all reasonable, and no particular energy minimum was favored. However, these results demonstrated the extensive mobility of the PEG linker that may ultimately provide an explanation for the observed activity data.

MICs and MBCs. MIC values for all polymerizable vancomycin derivatives were increased ($P < 0.08$ for all comparisons) relative to vancomycin, ranging from $7 \pm 1 \mu\text{M}$ to $67 \pm 20 \mu\text{M}$ (Table 2). MBC values were similarly increased. In general, the intuitive interpretations from Table 2 were correct. The specifics are as follows: the VA-1 MIC was less than the VA-2 MIC ($P = 0.01$); the VA-1 MIC was not statistically different from the VPA(3400) MIC ($P = 1$), but was less than the VPA(5000) MIC ($P = 0.05$); the VA-2 MIC was higher than the VPA(3400) MIC ($P = 0.03$), but was not statistically different from the VPA(5000) MIC ($P = 0.14$); and the VPA(3400) MIC was less than the VPA(5000) MIC ($P = 0.08$). MBC comparisons were analogous. Of note is that the VA-1 MBC was statistically greater than its MIC ($P = 0.05$). VA-2 showed a similar result ($P = 0.03$). However, the VPA(3400) MBC was not statistically greater than its MIC ($P = 0.3$), nor was there a difference for the VPA(5000) pair.

The 2D NMR data described above offers a unique opportunity to correlate antibiotic activity data in the form of MIC values with known biochemical structural relationships. Data strongly suggest that the decreased activity observed with VA-2 versus VA-1 (MIC of $39 \mu\text{M}$ versus $7 \mu\text{M}$, respectively) is the result of interference with a single hydrogen bond normally made with bacterial peptidoglycan D-Ala-D-Ala. The acrylamide carbonyl oxygen of VA-2 is placed within only a few angstroms of a vancomycin amide important for H-bonding bacterial peptidoglycan precursors. It is likely that this conformation allows for competitive, intramolecular blocking of D-Ala-D-Ala binding (Figure 9A). This hypothesis is substantiated by molecular dynamics results, which show a conformational energy minimum when the acrylamide oxygen assumes a position ca. 2.0 Å from this vancomycin amide hydrogen, a typical bond distance for amide–amide hydrogen bonds.

More complicated is the observed difference in activity between VA-1 and vancomycin (both modified at the glycosidic primary amine). The decreased activity of VA-1 is most likely explained in terms of interference with sugar-mediated dimerization whereby the acrylamide makes it sterically more difficult to form favorable interactions (Figure 9B). It is well-established that interactions between glycopeptide sugars play a role in stabilizing dimers,^{33–35,37} and it has been suggested that the vancomycin glucose units interact hydrophobically via axial C–H groups (Figure 1C, 9B).³⁵ It has been demonstrated, for example, that adding groups such as di- or tribenzene functionalities to the glycosidic primary amine of certain glycopeptide antibiotics, presumably facilitating hydrophobic interactions, can increase the potency of these species.⁷² Moreover, Kannan et al. demonstrated that acetylation of vancomycin at the glycosidic primary amine decreases antibacterial activity by approximately a factor of 12 but only decreases binding affinity to an Ac₂-L-Lys-D-Ala-D-Ala ligand (an analog of bacterial peptidoglycan) by a factor of 3.⁷³ These results suggest that modification of the sugar residue does not interfere with the vancomycin binding pocket but does alter the dimerization constant. We observed approximately a 6-fold decrease in activity with VA-1, which is in reasonable agreement considering Kannan used a different bacterial species and activity assay.

The length of the PEG linker used to connect vancomycin to a polymerizable moiety also influences activity. The MIC value for VPA(5000) was significantly higher than that of VPA(3400),

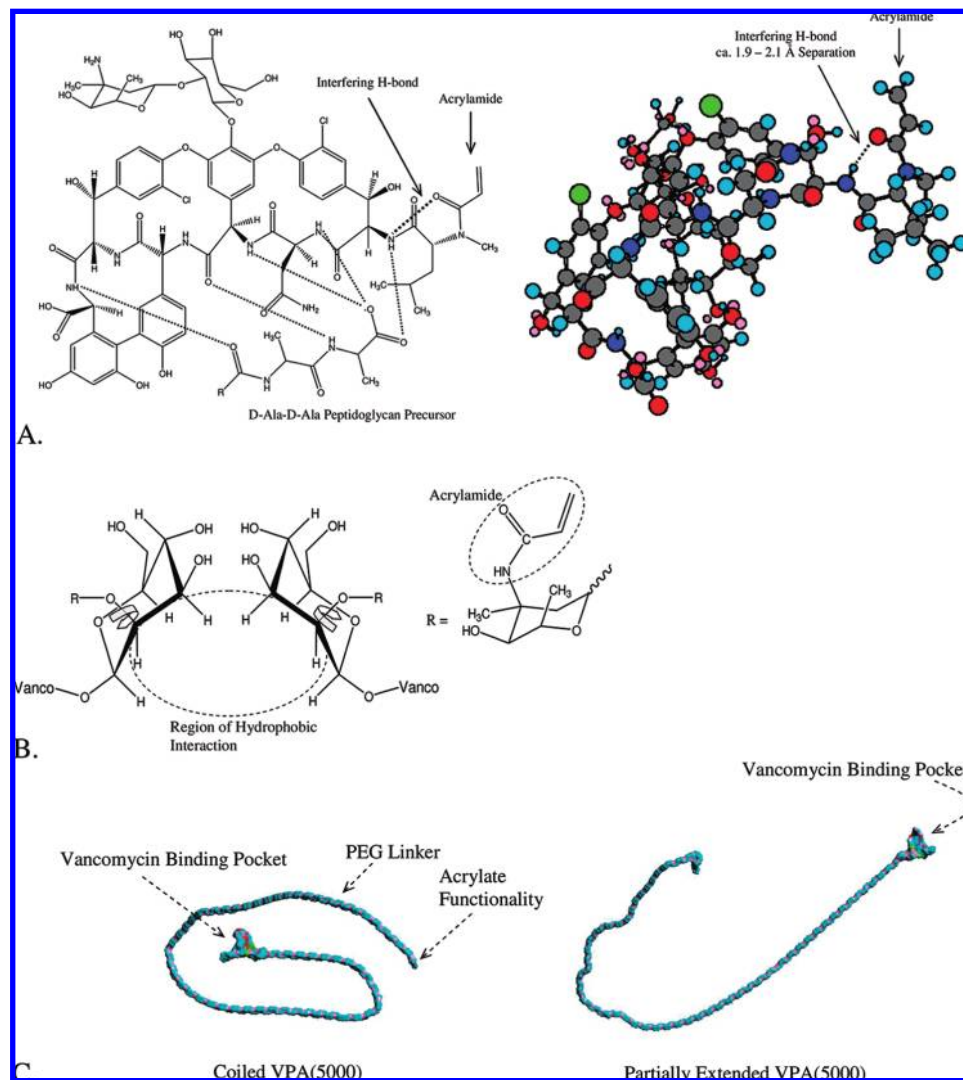


Figure 9. There are several possible mechanisms by which functionalization of vancomycin may decrease activity. (A) In the case of VA-2 (X_1 functionalization), competitive, intramolecular interference with an hydrogen-bond important for binding bacterial D-Ala-D-Ala is probable based on molecular dynamics calculations. (B) VA-1 (V_3 functionalization) may sterically interfere with glucose units important for dimer stabilization. Rotation about the illustrated bond could allow such interference. (C) PEG-acrylation of vancomycin at the V_3 position may decrease activity by blocking dimerization and/or by interfering with the vancomycin binding pocket (coiled structure). MIC data suggest the latter is dependent on PEG chain length. A partially extended VPA(5000) structure is shown for comparison. The Connolly molecular surfaces are drawn to scale, and the vancomycin head has a molecular diameter of ca. 20 Å.

Table 2. A Summary of MIC and MBC Data^a

antibacterial	MIC (μM)	MBC (μM)	fold decreased activity ^b
vancomycin	$1.1 \pm 0.1, n = 3$	MIC = MBC	1
VA-1	$7 \pm 1, n = 4$	$17 \pm 4, n = 3$	6.4
VA-2	$39 \pm 4, n = 6$	$60 \pm 5, n = 3$	35
vancomycin-PEG(3400)-acrylate	$7 \pm 1, n = 3$	$9 \pm 2, n = 3$	6.4
vancomycin-PEG(5000)-acrylate	$67 \pm 20, n = 3$	$75 \pm 25, n = 3$	61

^a In general, the intuitive comparisons are statistically correct. Functionalization at the V_3 or X_1 position decreases activity relative to vancomycin. However, modification at the X_1 site has a more pronounced effect (VA-2 vs VA-1). Increasing the length of the PEG linker also appears to decrease activity, presumably after some critical length is passed.

^b Ratio of MIC to the MIC of vancomycin.

Table 3. Various Copolymers of Polymerizable Antibiotic (Abx) and PEG(375)-Acrylate^a

Abx monomer	copolymer molar ratios		log reduction ^b
	Abx:PEG(375)-Acrl		
VPA(3400)	1:60	$7.0 \pm 0.4, n = 4$	
	1:175	$2 \pm 1, n = 4$	
VPA(5000)	1:60	$8 \pm 1, n = 4$	
	1:175	$0.0 \pm 0.3, n = 4$	
VA-1	1:20	$0.2 \pm 0.4, n = 4$	
	1:330	$0.3 \pm 0.3, n = 4$	
VA-2	1:20	$0.0 \pm 0.5, n = 5$	
	1:330	$0.5 \pm 1, n = 4$	

^a The monomer ratios are shown, which provide an approximation of the spacing between pendant vancomycin molecules along the polymer backbone. Here, the log reduction in bacterial numbers with respect to control surfaces [homopolymer of PEG(375)-acrylate] are shown. Of note is that only the PEG(X)-acrylate vancomycin derivatives showed surface antibacterial activity. Surfaces were inoculated with approximately 1×10^4 CFU/mL *S. epidermidis* ATCC 12228 and grown at 37°C for 20 h. Final bacterial concentration on control surfaces typically reached 1×10^7 CFU/mL to 1×10^8 CFU/mL. ^b If log reduction = 7, then the number of bacteria was reduced by 7 orders of magnitude with respect to the control surface.

indicating decreased activity of the former. One might consider degradative processes such as hydrolysis (enzymatic or otherwise) and the resultant fragmentary products when analyzing this differential activity. However, *Staphylococcus spp.* are not known to be PEG degraders,⁶⁰ and MIC values for species

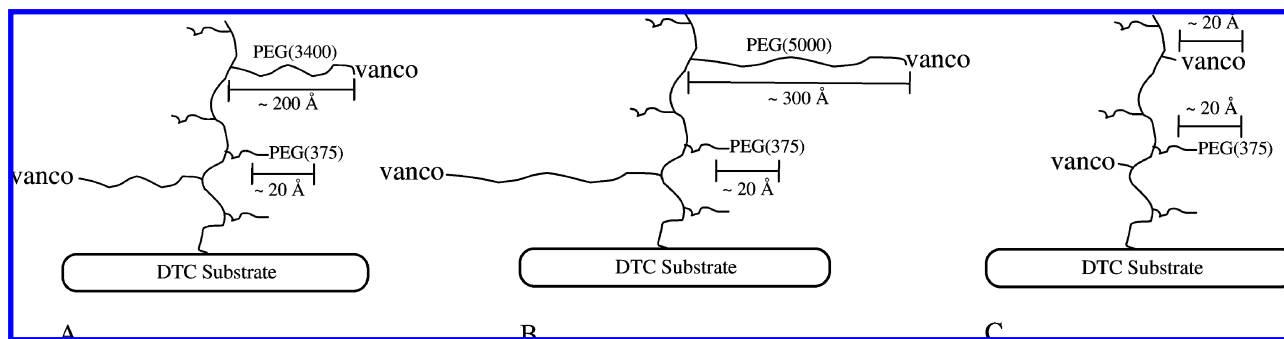


Figure 10. (A,B) When VPA(X) species are tethered from a surface pendant to a polyacrylate backbone, the translational degrees of freedom of the PEG chain will be reduced, potentially restoring antibacterial activity and facilitating desired biochemical interactions. (C) When VA-1 or VA-2 are copolymerized with PEG(375)-acrylate, it is expected that the pendant PEG moieties will block vancomycin interactions with D-Ala-D-Ala.

resulting from simple hydrolysis are likely to be quite large and computationally insignificant as noted previously. However, enzymatic ester hydrolysis of certain polymeric dental resins has been noted,⁷⁴ and suggests that issues related to degradation deserve future exploration. While the mobility of a PEG tether may ultimately be useful for facilitating interactions with bacterial cells when a polymerizable antibiotic (or other biomolecule) is covalently bound to a surface, that same PEG mobility may actually lead to twisted and convoluted geometries that shield the antibiotic from its binding target (Figure 9C) or interfere with higher-order structures such as dimers. Molecular dynamics simulations suggest a vast set of energetically favorable geometries encompassing the vancomycin moiety and the attached PEG chain, and it naturally follows that the longer the chain, the more varied the available conformational space. It appears that lengthening the PEG chain by approximately 50% from ca. 3400 Da to 5000 Da decreases relative activity by almost an order of magnitude in solution-based assays. This result suggests that the 5000 Da PEG chain may be of sufficient length to interfere with dimerization *and* to block D-Ala-D-Ala interactions in the vancomycin binding pocket, whereas the 3400 Da PEG chain may only interfere with the former.

Surface-Based Polymer Activity. VPA(3400) when copolymerized with PEG(375)-acrylate demonstrated bactericidal activity when the ratio of VPA(3400):PEG(375)-acrylate in the comonomer solution was ~1:60. Previous results suggest that a ratio of ~1:100 is bactericidal as well.²⁹ To a first approximation, the former ratio implies that, along the newly formed polymer backbone (polyacrylate backbone), there are approximately 60 pendant PEG(375) units for every pendant PEG(3400)-vancomycin species (Figure 5C), assuming random polymerization of the two monomers.

The photolithographic technique employed here is a convenient platform for constructing copolymers and for rapidly assessing their antibacterial properties. The expected polymer homogeneity in conjunction with improved spatial and temporal control of surface architectures is desirable for clarifying structural issues related to antibacterial action. In experiments described above, relative ratios of comonomers were varied to change the spacing of active antibiotic species along the resulting polymer backbone. Other parameters including polymer backbone length, the nature of the comonomer pendant functionality, and the hydrophobicity/hydrophilicity of the tether arm used for antibiotic conjugation deserve further exploration, in principle by the techniques described here. Experiments were also conducted with different polymerizable vancomycin derivatives both with and without PEG linkers to explore the importance of spatially

separating the active antibacterial moiety from the underlying polymer architectures. The site at which the vancomycin molecule was derivatized was also explored with two vancomycin acrylamide derivatives at the surface interface level.

For a given antibiotic monomer, a critical copolymer composition that defines bactericidal activity is expected, just as there is a critical solution concentration that defines MIC values. That ratio has not been tightly defined for the species presented here, but it has been determined with sufficient precision to relate surface-based and solution-based activity of monomers. Although VPA(5000) has a MIC approximately an order of magnitude higher than that of VPA(3400), it shows surface-based bactericidal activity at approximately the same graft composition (Table 3).

This could be the result of multiple biochemical interactions including (1) decreasing the translational degrees of freedom of the PEG chain through surface tethering, thus making the antibiotic binding pocket more accessible; (2) separating the vancomycin moiety from underlying, interfering polymer architectures (Figure 10); (3) simulating cooperative binding effects, as proposed with conventional vancomycin dimers,³³ by increasing the effective local antibiotic concentration; or (4) allowing the vancomycin molecule to penetrate some critical distance into the bacterial peptidoglycan layer. Grafts with VA-1 or VA-2 showed no surface-based activity. This may be related to structural features of the VA-1 and VA-2 monomers and their interaction with bacterial cells, or there may be differences in surface concentration related to steric effects encountered during polymerization. However, previous work has shown that acrylated IgG antibodies with no PEG spacer can be polymerized in a similar system,⁵⁶ as can methacrylated carboxyfluorescein diacetate.⁷⁵

Interestingly, the PEG tethers described here can extend between 200 Å [VPA(3400)] and 300 Å [VPA(5000)], and this distance corresponds closely to the thickness of the *Staphylococcal* peptidoglycan layer, which is typically 150–300 Å thick.⁷⁶ These mechanistic possibilities warrant further investigation.

As a final note, there is always concern that, when materials such as these are employed clinically, this could stimulate the development of antibiotic resistance. This issue has been addressed in part previously²⁹ with the addendum that the clinical situation would likely guide implementation. For example, these materials might be very useful for modifying orthopedic hardware when the bacterial load is not overwhelm-

ing but might be less appropriate in a polymicrobial, high bacterial load environment such as the oral cavity or gastrointestinal tract.

Conclusions

The facile synthesis, purification, and biochemical evaluation of various polymerizable vancomycin derivatives is presented with the intent of demonstrating a set of tools useful for evaluating new biomolecules engineered for surface modification of implantable biomaterials. Site specific modification of the parent antibiotic was achieved with either PEG-acrylate or acrylamide functionalities, and the site of modification was found to influence antibiotic activity. Consistent with well-established vancomycin mechanisms of action, molecular dynamics simulations in conjunction with MIC data suggest that interference with hydrogen bonds in the vancomycin binding pocket as well as interference with higher-order intermolecular complexes such as antibiotic dimers must be considered in the rational design of new polymerizable monomers. An iniferter-based surface-mediated polymerization was used to synthesize vancomycin-functionalized copolymers, and the nature of the tether separating the parent antibiotic from the attached polymerizable functionality affected the antibiotic activity. Monotonically decreasing activity was observed with increased PEG spacer length in solution-based MIC assays; however, experiments with polymerized vancomycin derivatives suggest that PEG tethers may be useful for separating the antibiotic moiety from other camouflaging polymer architectures and for spatially enabling desired biochemical interactions. Collectively, the data and techniques described above demonstrate the need for parsing structure–function relationships of polymerizable biomolecules intended for modifying biomaterial devices and for addressing specific design features of clinical import.

Acknowledgment. The authors wish to acknowledge the National Science Foundation for partial support of this research through Grant DE16523, and the U.S. Department of Education for a GAANN fellowship to M.C.L.

References and Notes

- Frommelt, L., Periprosthetic infection: Bacteria and the interface between prosthesis and bone. In *Interfaces in Total Hip Arthroplasties*; Learmouth, I. D., Ed.; Springer: London, 2000; pp 153–161.
- Balasundaram, G.; Webster, T. J. *Macromol. Biosci.* **2007**, *7* (5), 635–642.
- Christenson, E. M.; Anseth, K. S.; van den Beucken, J. J.; Chan, C. K.; Ercan, B.; Jansen, J. A.; Laurencin, C. T.; Li, W. J.; Murugan, R.; Nair, L. S.; Ramakrishna, S.; Tuan, R. S.; Webster, T. J.; Mikos, A. G. *J. Orthop. Res.* **2007**, *25* (1), 11–22.
- Tasker, L. H.; Sparey-Taylor, G. J.; Nokes, L. D. *Clin. Orthop. Relat. Res.* **2007**, *456*, 243–249.
- Popa, A.; Davidescu, C. M.; Trif, R.; Ilia, G.; Iliescu, S.; Dehelean, G. *React. Funct. Polym.* **2003**, *55* (2), 151–158.
- Kanazawa, A.; Ikeda, T.; Endo, T. *J. Appl. Polym. Sci.* **1994**, *53* (9), 1237–1244.
- Worley, S. D.; Sun, G. *Trends Polym. Sci.* **1996**, *4* (11), 364–370.
- Ikeda, T.; Hirayama, H.; Yamaguchi, H.; Tazuke, S.; Watanabe, M. *Antimicrob. Agents Chemother.* **1986**, *30* (1), 132–136.
- Tiller, J. C.; Liao, C. J.; Lewis, K.; Klibanov, A. M. *Proc. Natl. Acad. Sci. U.S.A.* **2001**, *98* (11), 5981–5985.
- Lu, G. Q.; Wu, D. C.; Fu, R. W. *React. Funct. Polym.* **2007**, *67* (4), 355–366.
- Gao, B. J.; Zhang, X.; Zhu, Y. *J. Biomater. Sci., Polym. Ed.* **2007**, *18* (5), 531–544.
- Nonaka, T.; Uemura, Y.; Ohse, K.; Jyono, K.; Kurihara, S. *J. Appl. Polym. Sci.* **1997**, *66* (8), 1621–1630.
- Kaya, I.; Bilici, A.; Sacak, M. *J. Appl. Polym. Sci.* **2006**, *102* (4), 3327–3333.
- Park, E. S.; Moon, W. S.; Song, M. J.; Kim, M. N.; Chung, K. H.; Yoon, J. S. *Int. Biodeterior. Biodegrad.* **2001**, *47* (4), 209–214.
- Lim, S. H.; Hudson, S. M. *Carbohydr. Res.* **2004**, *339* (2), 313–319.
- Huh, M. W.; Kang, I. K.; Lee, D. H.; Kim, W. S.; Lee, D. H.; Park, L. S.; Min, K. E.; Seo, K. H. *J. Appl. Polym. Sci.* **2001**, *81* (11), 2769–2778.
- Barnes, K.; Liang, J.; Worley, S. D.; Lee, J.; Broughton, R. M.; Huang, T. S. *J. Appl. Polym. Sci.* **2007**, *105* (4), 2306–2313.
- Liang, J.; Wu, R.; Huang, T. S.; Worley, S. D. *J. Appl. Polym. Sci.* **2005**, *97* (3), 1161–1166.
- Liang, J.; Wu, R.; Wang, J. W.; Barnes, K.; Worley, S. D.; Cho, U.; Lee, J.; Broughton, R. M.; Huang, T. S. *J. Ind. Microbiol. Biotechnol.* **2007**, *34* (2), 157–163.
- Luo, J.; Chen, Z.; Sun, Y. *J. Biomed. Mater. Res. A* **2006**, *77* (4), 823–831.
- Dizman, B.; Elasmri, M. O.; Mathias, L. J. *Biomacromolecules* **2005**, *6* (1), 514–520.
- Moon, W.-S.; Kim, J. C.; Chung, K.-H.; Park, E.-S.; Kim, M.-N.; Yoon, J.-S. *J. Appl. Polym. Sci.* **2002**, *90*, 1797–1801.
- Woo, G. L.; Mittelman, M. W.; Santerre, J. P. *Biomaterials* **2000**, *21* (12), 1235–1246.
- Woo, G. L.; Yang, M. L.; Yin, H. Q.; Jaffer, F.; Mittelman, M. W.; Santerre, J. P. *J. Biomed. Mater. Res.* **2002**, *59* (1), 35–45.
- Moon, W.-S.; Chung, K.-H.; Seol, D. J.; Park, E.-S.; Shim, J.-H.; Kim, M.-N.; Yoon, J.-S. *J. Appl. Polym. Sci.* **2003**, *90*, 2933–2937.
- Park, E.-S.; Lee, H.-J.; Park, H. Y.; Kim, M.-N.; Chung, K.-H.; Yoon, J.-S. *J. Appl. Polym. Sci.* **2000**, *80*, 728–736.
- Thamizharasi, S.; Vasantha, J.; Reddy, B. S. R. *Eur. Polym. J.* **2002**, *38* (3), 551–559.
- Patel, J. S.; Patel, S. V.; Talpada, N. P.; Patel, H. A. *Angew. Makromol. Chem.* **1999**, *271*, 24–27.
- Lawson, M. C.; Bowman, C. N.; Anseth, K. S. *Clin. Orthop. Relat. Res.* **2007**, *461*, 96–105.
- Arimoto, H.; Nishimura, K.; Kinumi, T.; Hayakawa, I.; Uemura, D. *Chem. Commun.* **1999**, *15*, 1361–1362.
- Arimoto, H.; Oishi, T.; Nishijima, M.; Kinumi, T. *Tetrahedron Lett.* **2001**, *42*, 3347–3350.
- Boneca, I. G.; Chiosis, G. *Expert Opin. Ther. Targets* **2003**, *7* (3), 311–328.
- Loll, P. J.; Axelsen, P. H. *Annu. Rev. Biophys. Biomol. Struct.* **2000**, *29*, 265–289.
- Williams, D. H.; Maguire, A. J.; Tsuzuki, W.; Westwell, M. S. *Science* **1998**, *280* (5364), 711–714.
- Williams, D. H.; Searle, M. S.; Mackay, J. P.; Gerhard, U.; Maplestone, R. A. *Proc. Natl. Acad. Sci. U.S.A.* **1993**, *90* (4), 1172–1178.
- Waltho, J. P.; Williams, D. H. *J. Am. Chem. Soc.* **1989**, *111* (7), 2475–2480.
- Gerhard, U.; Mackay, J. P.; Maplestone, R. A.; Williams, D. H. *J. Am. Chem. Soc.* **1993**, *115*, 232–237.
- Diana, J.; Visky, D.; Hoogmartens, J.; Van Schepdael, A.; Adams, E. *Rapid Commun. Mass Spectrom.* **2006**, *20* (4), 685–693.
- Griffin, J. H.; Linsell, M. S.; Nodwell, M. B.; Chen, Q. Q.; Pace, J. L.; Quast, K. L.; Krause, K. M.; Farrington, L.; Wu, T. X.; Higgins, D. L.; Jenkins, T. E.; Christensen, B. G.; Judice, J. K. *J. Am. Chem. Soc.* **2003**, *125* (21), 6517–6531.
- Johnson, A. W.; Smith, R. M. *J. Antibiot.* **1972**, *25* (5), 292–297.
- Nakamura, K.; Nishiyama, S.; Yamamura, S. *Tetrahedron Lett.* **1995**, *36* (47), 8625–8628.
- Nakamura, K.; Nishiyama, S.; Yamamura, S. *Tetrahedron Lett.* **1996**, *37* (2), 191–192.
- Nicolaou, K. C.; Hughes, R.; Cho, S. Y.; Winssinger, N.; Labischinski, H.; Endermann, R. *Chem.—Eur. J.* **2001**, *7* (17), 3824–3843.
- Popieniek, P. H.; Pratt, R. F. *J. Am. Chem. Soc.* **1991**, *113* (6), 2264–2270.
- Rao, J.; Yan, L.; Lahiri, J.; Whitesides, G. M.; Weis, R. M.; Warren, H. S. *Chem. Biol.* **1999**, *6* (6), 353–359.
- Williams, D. H.; Kalman, J. *J. Am. Chem. Soc.* **1977**, *99* (8), 2768–2774.
- Yao, N. H.; He, W. Y.; Lam, K. S.; Liu, G. *J. Comb. Chem.* **2005**, *7* (1), 123–129.
- Otsu, T.; Matsunaga, T.; Kuriyama, A.; Yoshioka, M. *Eur. Polym. J.* **1989**, *25*, 643–650.
- Otsu, T.; Kuriyama, A. *J. Macromol. Sci., Chem.* **1984**, *A21* (8–9), 961–977.
- Otsu, T.; Yoshida, M. *Polym. Bull.* **1982**, *7* (4), 197–203.
- Otsu, T.; Yoshida, M.; Kuriyama, A. *Polym. Bull.* **1982**, *7* (1), 45–50.
- Otsu, T.; Yoshida, M.; Tazaki, T. *Makromol. Chem., Rapid Commun.* **1982**, *3* (2), 133–140.

- (53) Harris, B. P.; Metters, A. T. *Macromolecules* **2006**, *39* (8), 2764–2772.
- (54) Kazmaier, P. M.; Moffat, K. A.; Georges, M. K.; Veregin, R. P. N.; Hamer, G. K. *Macromolecules* **1995**, *28* (6), 1841–1846.
- (55) Ishizu, K.; Khan, R. A.; Ohta, Y.; Furo, M. *J. Polym. Sci. Polym. Chem.* **2004**, *42* (1), 76–82.
- (56) Sebra, R. P.; Masters, K. S.; Bowman, C. N.; Anseth, K. S. *Langmuir* **2005**, *21* (24), 10907–10911.
- (57) Stewart, J. Approximate integration. In *Calculus*, 3rd ed.; Townes, K., Ed. Brooks/Cole Publishing Company: Pacific Grove, CA, 1995; pp 482–485.
- (58) Chirife, J.; Herszage, L.; Joseph, A.; Bozzini, J. P.; Leardini, N.; Kohn, E. S. *Antimicrob. Agents Chemother.* **1983**, *24*, 409–412.
- (59) Song, M.-J.; Kim, M.-N. *Int. Biodeterior. Biodegrad.* **2003**, *52*, 107–113.
- (60) Pan, L.; Gu, J.-D. *J. Polym. Environ.* **2006**, *15*, 57–65.
- (61) Harris, D. C. Propagation of uncertainty. In *Quantitative Chemical Analysis*, 4th ed.; W. H. Freeman and Company: China Lake, CA, 1996.
- (62) Hutchison, J. B.; Haraldsson, K. T.; Good, B. T.; Sebra, R. P.; Luo, N.; Anseth, K. S.; Bowman, C. N. *Lab. Chip* **2004**, *4* (6), 658–662.
- (63) Chen, L.; Wang, H.; Wang, J.; Chen, M.; Shang, L. *J. Biomed. Mater. Res. B* **2007**, *83* (2), 589–595.
- (64) Hanssen, A. D. *Clin. Orthop. Relat. Res.* **2005**, *437*, 91–96.
- (65) Mendez, J. A.; Abraham, G. A.; del Mar Fernandez, M.; Vazquez, B.; San Roman, J. *J. Biomed. Mater. Res.* **2002**, *61* (1), 66–74.
- (66) Prabhu, S.; Hossainy, S. *J. Biomed. Mater. Res. A* **2007**, *80* (3), 732–741.
- (67) Ryu, W. H.; Vyakarnam, M.; Greco, R. S.; Prinz, F. B.; Fasching, R. *J. Biomed. Microdevices* **2007**, *9* (6), 845–853.
- (68) Chua, P. H.; Neoh, K. G.; Kang, E. T.; Wang, W. *Biomaterials* **2008**, *29* (10), 1412–1421.
- (69) Parvizi, J.; Wickstrom, E.; Zeiger, A. R.; Adams, C. S.; Shapiro, I. M.; Purtill, J. J.; Sharkey, P. F.; Hozack, W. J.; Rothman, R. H.; Hickok, N. J. *Clin. Orthop. Relat. Res.* **2004**, *429*, 33–38.
- (70) Kenawy, E. R.; Worley, S. D.; Broughton, R. *Biomacromolecules* **2007**, *8* (5), 1359–1384.
- (71) Hermanson, G. T. Zero-length cross-linkers. In *Bioconjugate Techniques*, 1st ed.; Academic Press: Rockford, IL, 1996; pp 169–186.
- (72) Yoshida, O.; Yasukata, T.; Sumino, Y.; Munekage, T.; Narukawa, Y.; Nishitani, Y. *Bioorg. Med. Chem. Lett.* **2002**, *12* (21), 3027–3031.
- (73) Kannan, R.; Harris, C. M.; Harris, T. M.; Waltho, J. P.; Skelton, N. J.; Williams, D. H. *J. Am. Chem. Soc.* **1988**, *110* (9), 2946–2953.
- (74) Jaffer, F.; Finer, Y.; Santerre, J. P. *Biomaterials* **2002**, *23*, 1707–1719.
- (75) Sebra, R. P.; Reddy, S. K.; Masters, K. S.; Bowman, C. N.; Anseth, K. S. *Acta Biomater.* **2007**, *3* (2), 151–161.
- (76) Vollmer, W.; Blanot, D.; de Pedro, M. A. *FEMS Microbiol. Rev.* **2008**, *32* (2), 149–167.

BM900410A